Biomech Model Mechanobiol (2009) 8:253–262
DOI 10.1007/s10237-008-0131-4

Residual stress in the adult mouse brain

Gang Xu · Philip V. Bayly · Larry A. Taber

Received: 6 May 2008 / Accepted: 19 June 2008 / Published online: 24 July 2008

Abstract This work provides direct evidence that sustained tensile stress exists in white matter of the mature mouse brain. This finding has important implications for the mechanisms of brain development, as tension in neural axons has been hypothesized to drive cortical folding in the human brain. In addition, knowledge of residual stress is required to fully understand the mechanisms behind traumatic brain injury and changes in mechanical properties due to aging and disease. To estimate residual stress in the brain, we performed serial dissection experiments on 500-μm thick coronal slices from fresh adult mouse brains and developed finite element models for these experiments. Radial cuts were made either into cortical gray matter, or through the cortex and the underlying white matter tract composed of parallel neural axons. Cuts into cortical gray matter did not open, but cuts through both layers consistently opened at the point where the cut crossed the white matter. We infer that the cerebral white matter is under considerable tension in the circumferential direction in the coronal cerebral plane, parallel to most of the neural fibers, while the cerebral cortical gray matter is in compression. The models show that the observed deformation after cutting can be caused by more growth in the gray matter than in the white matter, with the estimated tensile stress in the white matter being on the order of 100–1,000 Pa.

G. Xu · P. V. Bayly · L. A. Taber (✉)
Department of Biomedical Engineering,
Washington University, One Brookings Drive,
Campus Box 1097, St Louis, MO 63130-4899, USA
e-mail: lat@wustl.edu

P. V. Bayly
Department of Mechanical, Aerospace, and Structural Engineering,
Washington University, St Louis, MO 63130, USA

Keywords Biomechanics · Morphogenesis · Cortical folding · Axon · Stiffness

1 Introduction

During human brain development, the cerebral cortex undergoes substantial folding, which leads to a highly convoluted brain surface. Proper cortical folding is critical to normal brain function, as anomalies in this process are linked to a number of disorders, including schizophrenia, autism, epilepsy, and mental retardation (Nordahl et al. 2007; Porter et al. 2002; Sallet et al. 2003; Welker 1990). Although intriguing neuroscientists for more than a century, the mechanisms of cortical folding remain incompletely understood.

Clearly, cortical folding involves biomechanical forces, and some researchers have speculated that folding results from stresses induced by differential or constrained growth (Richman et al. 1975). More recently, investigators have postulated that tension in neural axons of cerebral white matter causes specific folding patterns (Hilgetag and Barbas 2005, 2006; Van Essen 1997). However, while experiments have shown that axons originating from chick sensory neurons can sustain significant tension (Dennerll et al. 1989), axons from embryonic chick brain neurons sustain considerably less tension (Chada et al. 1997). Hence, it is uncertain if significant tension exists in axons in both the developing and mature brain.

The primary objective of this work is to determine whether residual stress exists in the brain and to explore the distributions and source of this stress, if it exists. In living tissues, residual stresses may arise from growth, remodeling, or active force generation by cytoskeletal components (Fung 1993, 1998). Here, we use a variation of the method commonly used to characterize residual stress in soft tissue,

whereby the tissue is cut and the resulting deformation measured as the stress is released (Fung 1993).

In this initial study, adult mouse brains were used. Although the brains of mice, unlike those of many large mammals, do not undergo cortical folding, they are widely used and readily available for brain tissue studies due to their well-documented structural and functional information. Indeed, mouse brains can develop aberrant folding patterns ex vivo if cortical growth is enhanced by lysophosphatidic acid (Kingsbury et al. 2003), making them a potential candidate for studying abnormal folding mechanisms. Because axon tension has been postulated to play a role in brain folding, we herein focus on the regions of the mouse brain that contain most of the cortical white matter. A typical coronal section of the mouse brain containing cerebral white matter (corpus callosum) has three major components: cortical gray matter, white matter tract, and inner gray matter of thalamus (Fig. 1c). Gray matter is composed of unmyelinated neurons, including nerve cell bodies, glial cells, and short nerve cell extensions. White matter is composed largely of myelinated nerve cell processes, or parallel axons. The white matter tract contains three well-recognized regions: corpus callosum, cingulum, and external capsule (Fig. 1c). White matter conducts signals between different regions of gray matter, and, in particular, the corpus callosum connects structurally the two cerebral hemispheres of the brain.

The results of the dissection experiments described below suggest that the cerebral white matter tract is under considerable tension in the circumferential direction in the coronal plane, parallel to most of the neural fibers, while the cerebral cortical gray matter is in compression. Using computational modeling, we investigated whether the tension in the white matter can be caused by gray matter growing at a faster rate than, and hence stretching, the white matter. A finite element model for a brain slice indicated that such differential growth can produce deformations that agree well with our cutting experiments. These results are consistent with the idea that cortical growth constrained by axonal tension causes brain folding.

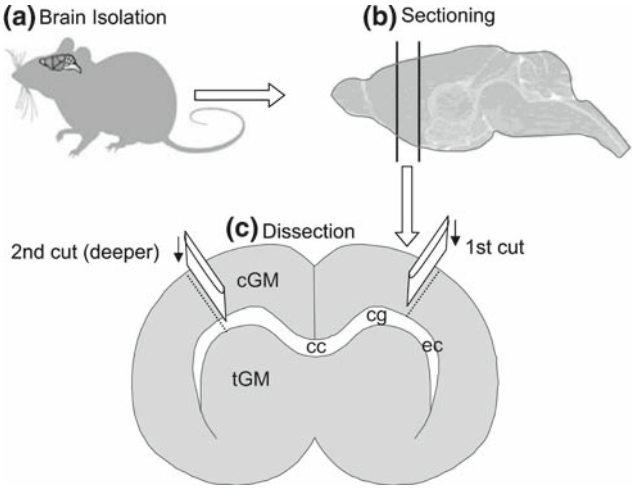

Fig. 1 Schematic of experimental procedure for mouse brain dissection (not drawn to scale). **a** The whole brain was removed from 12–15-week-old adult mice. **b** The brain was then mounted on the platform of a sectioning vibratome and 500-μm thick coronal slices were cut. **c** Only the slices containing corpus callosum were collected. A typical brain slice contains three major regions: cortical gray matter (*cGM*), thalamus gray matter (*tGM*), and white matter tract consisting of corpus callosum (*cc*), cingulum (*cg*), and external capsule (*ec*). In the experiments, a razor blade was used to make the first radial cut only through the cortical gray matter, and the second radial cut was made deeper through either the white matter tract or the inner gray matter of thalamus. The cartoons shown in **a** and **b** were adapted from http://pages.slc.edu/~krader/animals/index.htm, and http://www.hms.harvard.edu/research/brain/atlas.html, respectively

2 Materials and methods

2.1 Brain slice preparation

All animal procedures were approved by the Washington University Animal Studies Committee. We used 12–15-week-old adult female C57BL/6J mice (Jackson Laboratory, Bar Harbor, ME, USA). Methods were modified from a previous report for acute mouse brain slice preparation (Tekkok and Goldberg 2001). Briefly, each mouse ($n = 5$) was anesthetized with 5% isoflurane in air. The whole brain was immediately removed from the skull (Fig. 1a) and placed into ice-cold artificial cerebrospinal fluid (aCSF; 25 mM $NaHCO_3$, 122 mM NaCl, 1.3 mM $CaCl_2$, 1.2 mM $MgSO_4$, 3 mM KCl, and 0.4 mM KH_2PO_4; pH 7.35) (Alexander et al. 2000). The brain was then mounted on the platform of a sectioning vibratome (Vibratome 1000, Technical Products, St Louis, MO, USA) and 500-μm thick coronal slices were cut (Fig. 1b). In the sectioning process, the brain was immersed in ice-cold aCSF. Only the slices (about 8/brain) containing corpus callosum were collected and included in the following serial dissection experiments.

2.2 Tissue dissection

Brain slices were allowed to recover for about 15 min at room temperature (~22°C) in aCSF. To probe the circumferential (in the coronal plane) residual stresses in different cerebral layers, radial cuts were made with a razor blade completely through the slice thickness at three levels of depth into the brain (Fig. 1c): (1) through the cerebral cortical gray matter, (2) deeper into the white matter tract, and (3) further into inner gray matter of thalamus. The degree of opening at the cutting site served as an indicator of the magnitude of the residual stress in the circumferential direction. Tensile stresses would pull the cut open while compressive stress would keep the cut closed. To minimize tissue damage by the blade and ensure

a straight cut, only one cut at a specified depth was made at each location. To ensure clean cuts, a new blade was used for each brain. In general, radial cuts of different depths were made on each of two symmetric sides (hemispheres) of the same brain slice for comparison (Fig. 1c).

To probe the deformation caused by surrounding gray matter, some white matter tracts were isolated (with a small amount of residual gray matter) from intact brain slices. Inner gray matter was removed first by a series of small cuts with a pair of fine spring scissors (Fine Science Tools, Foster City, CA, USA). Most of the cortical gray matter was then removed by several straight cuts with a razor blade. The overall morphology of the cortical white matter tract was characterized by the angle (φ) between two radii joining the midpoint of the inner wall to the tips of the white matter tract (see Fig. 4a1, a2). To compare slices between different regions in different subjects, the measured angles were normalized relative to their original values from the intact brain slices ($\varphi^* = \varphi_{\text{cut}}/\varphi_{\text{intact}}$).

Each slice was imaged immediately and 15 min after each dissection with a video camera (COHU, Model 4915, San Diego, CA, USA) mounted on a dissecting microscope (Leica Microsystems, Model MZ8, Bannockburn, IL, USA). Images were acquired by a frame grabber (FlashBus MV, Integral Technologies, Indianapolis, IN, USA) and imaging software (SigmaScan Pro V.5.0, Systat Software, San Jose, CA, USA).

2.3 Finite element model

To explore the possible cause of tension in the white matter and to estimate the magnitude of the residual stress, a nonlinear finite element model for the mouse brain slice was created using the commercial finite element software COMSOL Multiphysics (V.3.3, COMSOL AB). Resembling the overall morphology of real mouse brain slices, the plane-stress model was composed of three layers representing cortical gray matter, white matter tract, and inner gray matter (Fig. 2a). Due to symmetry, only half of the slice needed to be analyzed. Symmetry conditions were always specified along the straight vertical boundary. To simulate a cut of specific depth, a thin (10-μm wide) rectangular region along the radial direction was removed (Fig. 2b). The model geometry was partitioned into triangular mesh elements in COMSOL (Fig. 2b). The mesh was further refined near the boundaries of the cut (see close-up of the regional mesh in Fig. 2c). The sufficiency of the mesh density was confirmed by solving the problem for increasing mesh densities.

We speculate that residual stress in the brain is generated by differential growth during development. Volumetric growth was modeled using the theory of Rodriguez et al. (1994). Briefly, starting with the zero-stress configuration, each material element grows according to a specified growth deformation gradient tensor $\mathbf{F}_g$. Maintaining geometric compatibility between elements generally requires elastic deformation $\mathbf{F}_e$ that causes stress. Thus, the total deformation is described by $\mathbf{F} = \mathbf{F}_e \cdot \mathbf{F}_g$, where $\mathbf{F}_g = \mathbf{I}$ for no net growth with $\mathbf{I}$ being the identity tensor. In our computations, the main deformation variable is $\mathbf{F}$, $\mathbf{F}_g$ is specified, and stress depends on $\mathbf{F}_e = \mathbf{F} \cdot \mathbf{F}_g^{-1}$. In the current models, we considered only isotropic growth with $\mathbf{F}_g = \lambda_g \mathbf{I}$, where λ_g is the growth 'stretch ratio' (Taber and Perucchio 2000; Taber 2001).

To a first approximation, both gray matter and white matter are assumed to be isotropic, nearly incompressible, pseudoelastic materials characterized by the modified neo-Hookean strain-energy density function $W = \frac{1}{2}\mu(I_1 J_e^{-\frac{2}{3}} - 3) + p(1 - J_e - \frac{p}{2\kappa})$, where μ and κ are the shear and bulk modulus, respectively, I_1 is the first invariant of the right Cauchy–Green deformation tensor (given by $\mathbf{F}_e^{\mathrm{T}} \cdot \mathbf{F}_e$), $J_e = \det \mathbf{F}_e$ is the elastic volume ratio, and p is a penalty variable introduced for nearly incompressible materials. The Cauchy stress tensor is given by the constitutive relation $\boldsymbol{\sigma} = J_e^{-1} \mathbf{F}_e \cdot \partial W / \partial \mathbf{F}_e^{\mathrm{T}}$. More details on the implementation of growth in COMSOL are given in Taber (2007).

Because regional material properties during growth have not yet been measured in the mouse brain, we assume that the constitutive relations and growth are uniform throughout the white and gray matter, although the modulus and growth magnitudes can differ. In fact, for nearly incompressible materials, the behavior of the model depends only on the ratios $\mu^* = \mu_G/\mu_W$ and $\lambda_g^* = \lambda_{gG}/\lambda_{gW}$, where the subscripts W and G denote white and gray matter, respectively. Hence, the specified differential growth ($\lambda_g^* \neq 1$) is the only driving force in the model. (For $\lambda_g^* = 1$, no residual stresses develop even when $\mu^* \neq 1$.) The values of these parameters and how they affect the results are discussed below.

Residual stresses also are normalized relative to the white matter shear modulus ($\sigma_\theta^* = \sigma_\theta/\mu_W$). Moreover, simulations revealed that when κ is large relative to μ, i.e., the material is nearly incompressible, the results are relatively insensitive to the value of the bulk modulus. For numerical stability, we took κ to be about six orders of magnitude larger than μ for both white and gray matter.

3 Results

3.1 Gray matter is in compression and white matter tract is in tension

Following a radial cut in the cortical gray matter, the cut did not open (Fig. 3a2, b2). This behavior was consistent for all the coronal brain slices (containing corpus callosum) from the adult mouse ($n = 5$). This result indicates the presence of little residual stress or compressive stress in the

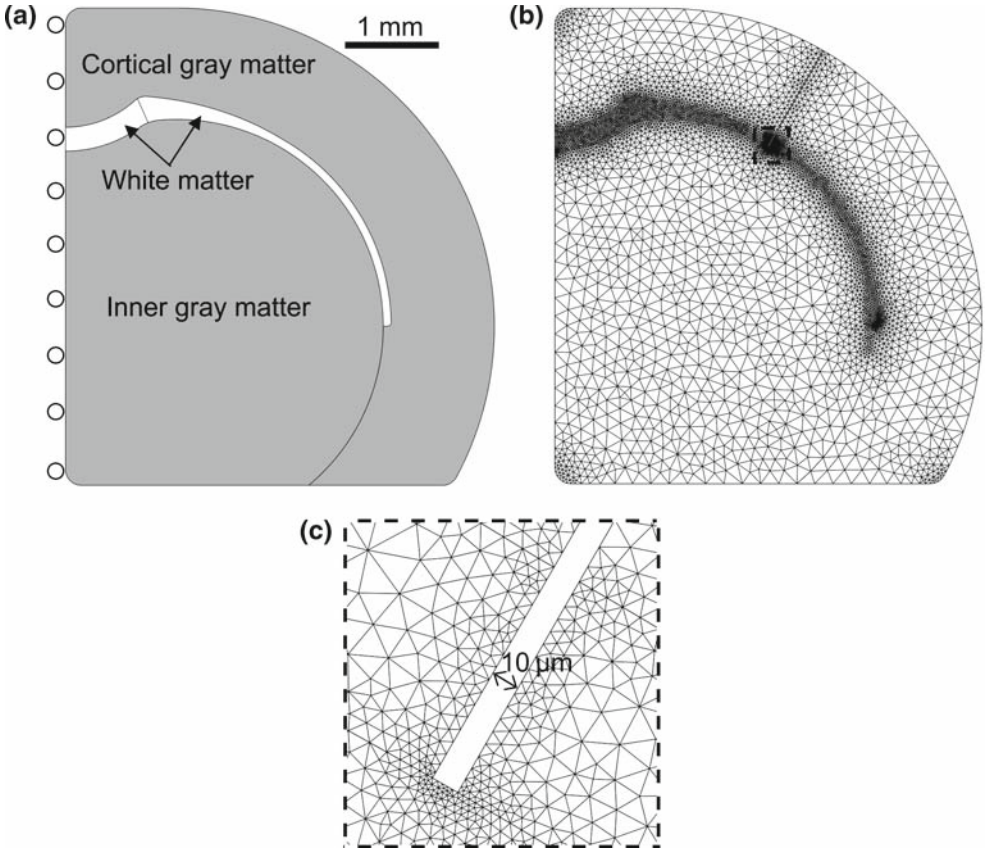

Fig. 2 Finite element model for the mouse brain in the coronal plane. **a** Schematic of model for intact brain slice. Due to symmetry, only half of the slice is analyzed. Symmetry conditions (represented by rollers) are specified along the straight vertical boundary (one point was fixed). Other boundaries are free. **b** Model geometry partitioned into triangular mesh elements. A narrow cut is simulated by removing a thin (10-μm wide) rectangular region. Note denser mesh for the white matter track and the cut region. **c** Close-up of mesh near the cut (*dashed rectangle* in **b**)

circumferential direction of the coronal plane in the cortical gray matter of the intact slice.

Since little deformation occurred after the first cut, this cut likely had little effect on the stress distribution in the white matter tract and the rest of the brain tissue. Thus, another deeper cut was next made on the other side (hemisphere) of the brain slice (Fig. 3a3, b3). Cutting radially through both the cortical gray matter and the white matter tract resulted in considerable opening of the white matter tract in the circumferential direction (Fig. 3a3). The opening is a clear signature of tensile residual stresses in the circumferential direction in the coronal cerebral plane, parallel to the most of the neural fibers along the white matter tract (Larvaron et al. 2007; Olivares et al. 2001; Valverde 2004). The edges in the white matter tract from a straight cut always assumed a concave shape with a wider opening or separation in the middle of the tract and much smaller separation in the adjacent gray matter (Fig. 3a3). The largest cut separation distance was approximately 100 μm right after cutting (Fig. 3a3), and it became nearly twice as large after about 15 min (Fig. 3a4), illustrating the viscoelastic nature of living brain tissue. However, the cut in the cortical gray matter remained mostly closed (Fig. 3a3, a4), indicating the presence of compressive residual stresses in this region.

When deeper cuts were made into the inner gray matter of the thalamus, the inner gray matter opened considerably and resulted in wider opening of the white matter tract (Fig. 3b3). Similarly, these openings enlarged after about 15 min (Fig. 3b4), presumably due to viscoelastic deformation.

3.2 Stresses in white and gray matter are coupled

On a coronal slice of an adult mouse brain, the cortical white matter tract is relatively thick in the center region (corpus callosum) and gradually attenuates (cingulum and external capsule) in moving along the circumferential direction (Figs. 3a1, b1, 4a1). To examine the mechanical coupling between the white and gray matter, we removed most of the

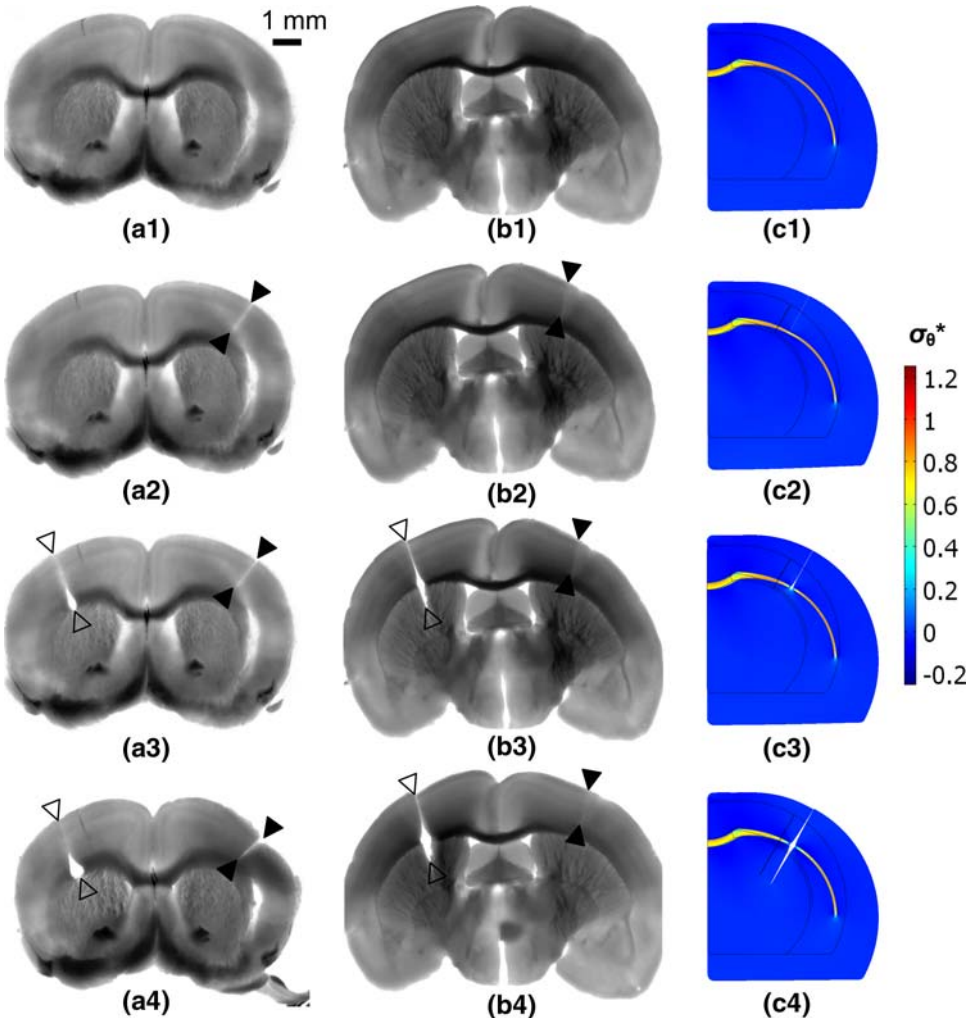

Fig. 3 Serial cuts made on a coronal slice of an adult mouse brain. **a1**, **b1** Brain slice obtained by vibratome sectioning. **a2**, **b2** The first radial cut (indicated by a pair of *solid arrowheads*) was made only through the cortical gray matter. The cut did not open. **a3**, **b3** The second radial cut (indicated by a pair of *open arrowheads*) was made through the underlying white matter tract (**a3**) or deeper into inner thalamus gray matter (**b3**). The cut opened at the site of the white matter tract or inner gray matter. **a4**, **b4** After about 15 min, the opening in the white matter tract became wider, but cuts through cortical gray matter stayed closed. The overall morphology of the slices in **a1** and **b1** is typical for the first and third corpus callosum-containing slices, respectively, obtained during coronal sectioning (from anterior to posterior part of the brain). **c1–c4** Normalized circumferential stress (σ_θ^*) distribution in finite element models for the dissection experiments ($\mu^* = 0.5$, $\lambda_g^* = 1.3$). Due to relatively more growth in gray matter, gray matter is in compression and white matter is in tension. Radial cuts were made into cortical gray matter (**c2**), white matter (**c3**), or inner gray matter (**c4**), respectively. The smaller outline shown in each plot is the same slice before growth

inner and cortical gray matter and examined how the overall shape (characterized by the angle φ defined in Fig. 4a1, a2) of the white matter tract changed. On average, the angle decreased by about 30% after removal of the gray matter ($\varphi^* = \varphi_{\text{cut}}/\varphi_{\text{intact}} = 0.67 \pm 0.04$; $p < 0.0001$; four slices from four mice) (see Fig. 4a1, a2). These results indicate that residual tension in the white matter is closely coupled with compression in the gray matter. Other noteworthy features include the change in curvature of the corpus callosum and the curved edges of the cortical gray matter following the straight cuts (Fig. 4a2).

3.3 Quantitative estimate of residual stress in white matter

The cutting experiments have demonstrated that residual stresses exist in both gray and white matter in the adult mouse brain. The white matter tract contains considerable tensile stress in the axonal fiber directions along the white matter tract in the coronal plane, while the gray matter is in a state of circumferential compression. To explore the possible source of these stresses, as well as to estimate their magnitude, we created finite element models for the above experiments (Figs. 3, 4). The overall morphology of our models (Figs. 3c1,

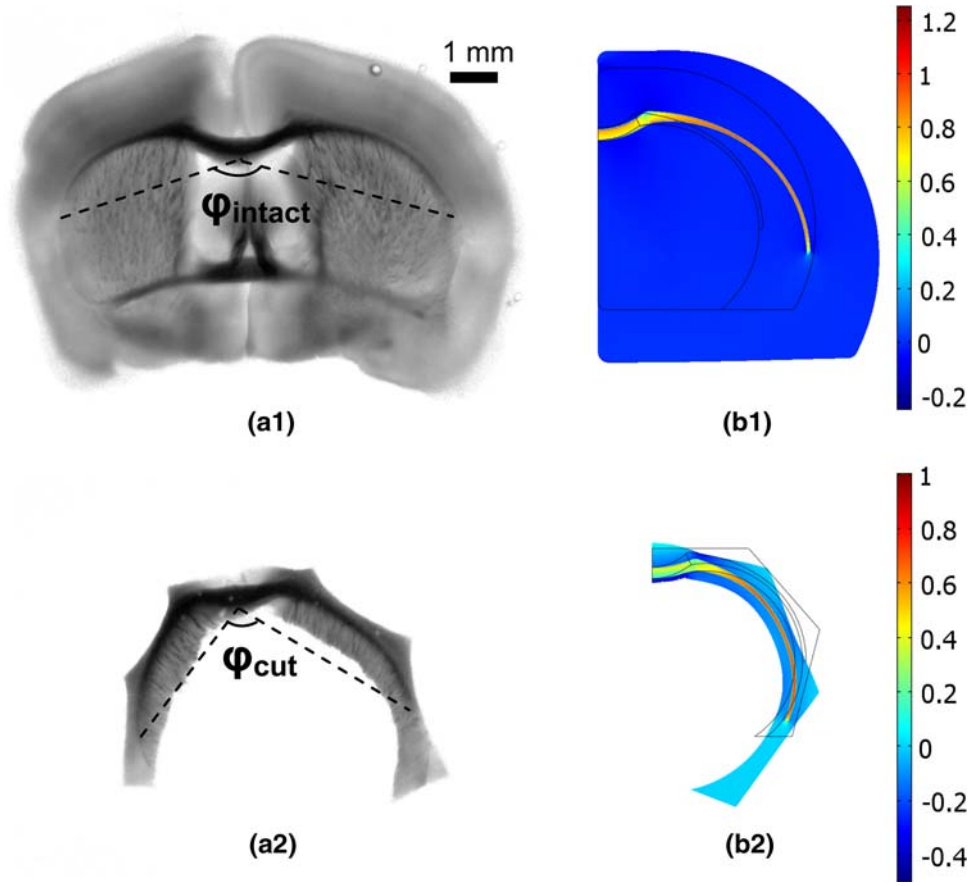

Fig. 4 White matter tract of mouse brain with and without the constraints of gray matter. **a1** Brain slice obtained by vibratome sectioning. The overall morphology is typical for a slice just posterior to the one shown in Fig. 3a1. The angle ($\varphi_{\text{intact}} = 150°$) characterizing the white matter tract is shown. **a2** Same slice with inner thalamus gray matter dissected away by scissors and cortical gray matter cut away with several straight cuts by a blade. In this specimen, the angle ($\varphi_{\text{cut}} = 99°$) of the white matter tract decreased by 33% ($\varphi^* = 0.66$) after these cuts. **b1**, **b2** Normalized circumferential stress distributions in finite element models before and after dissections. The model for the intact slice (**b1**) is the same as that in Fig. 3c1. Similar to the experimental result, after removal of the majority of the gray matter, the white matter angle decreased dramatically ($\varphi^* = 0.70$), and straight cuts on the cortical gray matter became curved (**b2**)

4b1) is similar to that of actual mouse brain slices (Figs. 3a1, b1, 4a1). The results in these figures are based on the parameter values $\mu^* = 0.5$ and $\lambda_g^* = 1.3$. (The effects of varying these parameters are discussed below.)

The results from the model indicate that differential growth can generate considerable residual stress with tension in white matter and compression in gray matter (Fig. 3c1). For the selected model parameters, simulating cuts of certain depths into the brain slice yields results in good agreement with those given by our cutting experiments (compare experimental and computational results for each row in Fig. 3). In addition, for nearly isolated white matter (with some remaining cortical gray matter), our model produces similar shapes (Fig. 4b2) to those in our experiments (see Fig. 4a2). The model further predicts the curved surfaces following straight cutting of the cortical gray matter. Taken together, these results indicate that differential growth between gray and white matter can generate the observed residual tension in the white matter tract.

Because of the wide range of material properties reported for brain tissue (see Table 1 of Thibault and Margulies 1998), and the lack of prior information on mechanical properties and growth in the mouse brain, we conducted a sensitivity analysis to examine the effects of the relative (gray/white) modulus (μ^*) and growth (λ_g^*) on the normalized angle (φ^*) and residual circumferential stress in the white matter tract. (The circumferential stress σ_θ^* represents the average value across the symmetry plane of the corpus callosum.) In general, φ^* decreases with increasing relative gray matter growth (λ_g^*) or decreasing relative modulus (μ^*), while σ_θ^* increases with increasing λ_g^* or increasing μ^* (Fig. 5). In other words, the larger the relative gray matter growth, the larger the change in the white matter angle after isolation and the larger the residual stress in the white matter in the intact slice. Also,

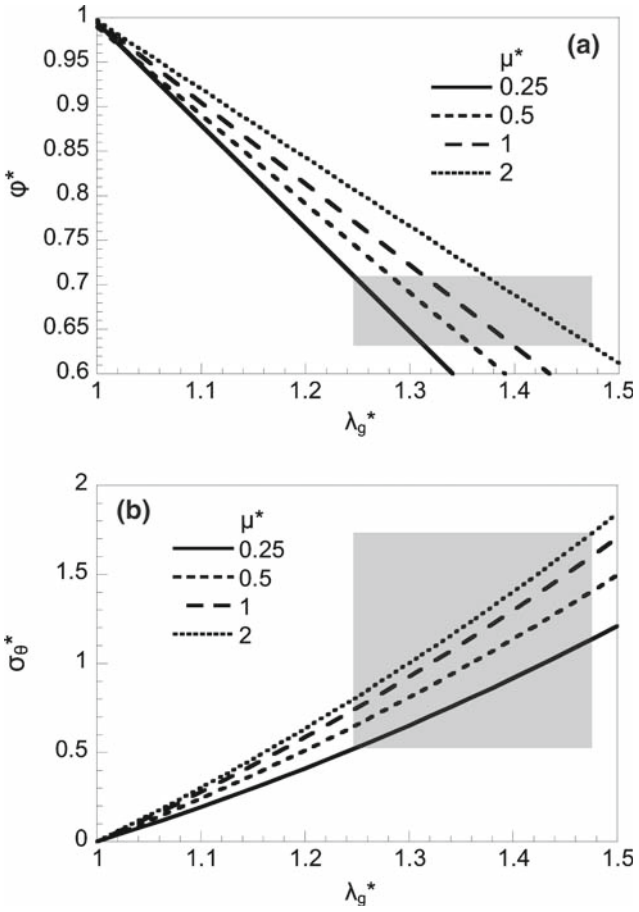

Fig. 5 Dependence of the normalized white matter tract angle (φ^*) and residual circumferential stress (σ_θ^*) in the white matter on relative growth (λ_g^*) and stiffness (μ^*) from the finite element model. **a** Dependence of φ^* on λ_g^* and μ^*. The shadowed area is the relative growth range for gray matter when the normalized white matter angle matches the experimental data ($\varphi^* = 0.67 \pm 0.04$). **b** Dependence of σ_θ^* on λ_g^* and μ^*. The white matter stress σ_θ^* represents the average value across the symmetry plane of the corpus callosum. The shadowed area corresponds to the same growth range for gray matter from **a** and covers the scope of expected residual stress level in the white matter

the larger the relative gray matter shear modulus, the smaller the change in the white matter angle after isolation (gray matter is harder to deform) and the larger the residual stress in the white matter in the intact slice (gray matter stretches white matter more easily).

To match the experimental value of φ^* (0.67) within one standard deviation after isolation (see Fig. 4a1, a2), the value of λ_g^* must fall in a relatively narrow range of about 1.25–1.47, which also depends on the value of μ^* (Fig. 5a). This is consistent with data showing that the increase in overall size of the mouse brain during postnatal maturation is roughly 20–30% (Larvaron et al. 2007). For this amount of growth, the value of σ_θ^* lies in the range of about 0.5–1.7, depending on the value of μ^* (Fig. 5b). Unfortunately, the mechanical properties of the mouse brain have not yet been measured. However, if we assume that the overall stiffness of white matter is similar to that of gray matter, as has been shown for the porcine brain ($\mu^* = \sim 1.3$) (Prange and Margulies 2002), then Fig. 5b indicates that the value of σ_θ^* likely is close to 1. Hence, if the mouse brain has properties similar to those of the rat brain, which has a bulk shear modulus of 100–1,000 Pa (Elkin et al. 2007; Gefen et al. 2003; Georges et al. 2006), then the residual stress ($\sigma_\theta = \mu_W \sigma_\theta^*$) in the mouse brain would be on the order of 100–1,000 Pa.

4 Discussion

In this work, we provide evidence that axons in the mature brain sustain considerable tension. Some investigators have speculated that axon tension plays a crucial role in cortical folding during brain development (Hilgetag and Barbas 2005, 2006; Van Essen 1997). One possibility is that axons constrain the expansion of local regions of the growing brain cortex, causing it to form specific folding patterns. Our findings support the feasibility of this idea. An important caveat, however, is that developing brains may have different mechanical properties than mature brains (Gefen et al. 2003).

Previous studies with single neurons have shown that developing axons can bear considerable axial tension (Lamoureux et al. 1989). In general, a chick sensory axon elongates and sustains tensile forces on the order of 100 μdyn (or 1 nN) when pulled by a needle (Dennerll et al. 1989; Lamoureux et al. 1989), while neurites from embryonic chick forebrain neurons apparently sustain much smaller tensile forces that are on the order of 10 μdyn (or 0.1 nN) (Chada et al. 1997). In addition, axons from hippocampal neurons of embryonic rats can also grow in response to tensions on the order of 10–100 μdyn (Lamoureux et al. 2002), although the magnitude of tensile force that these axons can maintain is unknown.

If we assume that axons in the mature mouse brain can sustain tensions similar to those for developing chick forebrain axons (0.1 nN), the stress can be estimated by noting that the diameter of axon fibers in the mammalian corpus callosum is conserved across species and is generally in the range of 0.1–1 μm (Faisal et al. 2005; Olivares et al. 2001). Hence, the magnitude of the tensile stress (force/area) in an axon of the adult mouse brain is in the range of 10^2–10^4 Pa. The tensile stress in the white matter tract from our finite element model (on the order of 100–1,000 Pa) agrees well with this estimate, suggesting that a similar level of stress may be maintained in axons in both the developing and mature central nervous system. The magnitude of the residual stress given by the models depends on the assigned material properties, as well as the specified growth in different regions. The parameter values used are based on available data in the literature, but these data are incomplete. The models, however, predict quite well the results from the cutting experiments (see Figs. 3, 4), suggesting that the chosen values are reasonable.

As a first approximation, our model includes isotropic growth of gray matter relative to white matter without any change of material properties. However, the material properties of the brain might change significantly during postnatal development or maturation due to alterations in water content and myelination of fiber tracts (Larvaron et al. 2007; Neil et al. 2002). Therefore, to refine our finite element models much work is needed to determine the regional material properties (and residual stresses) of the mouse brain at different developmental stages.

Our experiments indicate that, while the white matter tract is in tension, the cortical plate and inner region of gray matter are in a state of compression in the circumferential direction in the coronal cerebral plane. The results from our finite element models agree with this conclusion (Fig. 3). In addition, stresses in different regions are closely coupled as manifested by the significant change of the white matter angle after isolation from the brain slice (Fig. 4). Equilibrium of an unloaded object requires that tension in some regions must be balanced by compression in other regions. Thus, there may be no physiological reason for the compression in the gray matter. However, from a mechanics perspective, the coupling between tension in white matter and compression in gray matter may provide superior structural stability for normal brain functioning, as the white matter tract connects structurally the two cerebral hemispheres of the brain. This finding is also relevant to studies on traumatic brain injury that use mouse brain models.

In addition to differential growth, tension in axons could be generated by active contraction. However, myosin-based cytoskeletal contraction is likely minimal in most white matter of the adult mouse brain due to relatively low levels of myosin II in this region (Kioussi 2007; Miller et al. 1992). Hence, differential growth is the more likely mechanism. This conclusion agrees with previous speculation by Richman et al. (1975), as well as recent experiments showing that accelerated growth can lead to aberrant folding in the mouse brain (Kingsbury et al. 2003).

Quantitative biomechanical models for the brain, like those used in this work, are useful for testing theories for cortical folding (Richman et al. 1975; Todd 1982; Toro and Burnod 2005; Van Essen 1997). In addition, there is an increasing demand for computational models in the areas of neurosurgery (Kyriacou et al. 2002; Miller 1999) and traumatic brain injury (Zhang et al. 2001), where material properties of brain tissue change due to injury, aging, and diseases (Drapaca et al. 2006; Gefen et al. 2003; Prange and Margulies 2002; Taylor and Miller 2004; Thibault and Margulies 1998). Mechanical properties of brain tissues are needed for these models. Accurate determination of these properties requires knowledge of the zero-stress state of the tissue (Fung 1993; Zamir and Taber 2004). Residual stress also can greatly affect the stress distributions in loaded tissue (Fung 1998), e.g., during impact.

To date, however, residual stresses have generally been ignored in studies of brain biomechanics. Material properties for various animal brains have been reported using conventional testing methods such as shear (Coats and Margulies 2006; Georges et al. 2006; Hrapko et al. 2006; Prange and Margulies 2002; Thibault and Margulies 1998), compression (Cheng and Bilston 2007; Elkin et al. 2007; Miller 1999; Miller and Chinzei 1997; Prange and Margulies 2002), indentation (Elkin et al. 2007; Gefen et al. 2003; Gefen and Margulies 2004; Miller et al. 2000), and extension (Miller and Chinzei 2002). These measurements have been performed on either the whole brain or certain regions of the brain. However, residual stress has been ignored in all of these reports. The present study provides information that can be used to improve these measurements of material properties.

Limitations in our models mainly reside in the assumptions regarding material properties. First, white matter probably is better modeled as a transversely isotropic material due to the orientation of neural fibers. Second, although better than linear elasticity on which many reported measurements are based, a neo-Hookean material may not be an accurate representation for mouse brain tissue. Indeed, other forms of strain-energy density function for brain tissue have been proposed in the literature, e.g., the first order Ogden hyperelastic material for the porcine brain (Coats and Margulies 2006; Prange and Margulies 2002). Third, material properties may vary regionally within gray or white matter. Finally, brain tissue is clearly viscoelastic, as demonstrated by the time-dependent changes after cutting (Fig. 3a4, b4). To address these issues, as well as to improve our model, further mechanical testing on regional material properties of the mouse brain is needed.

In conclusion, we have found that the adult mouse brain contains significant residual stress. The white matter tract and gray matter are in states of tension and compression, respectively, in the circumferential direction in the coronal cerebral plane. These results could have important implications for studies of brain folding, mechanical properties, and injury due to trauma. We hope this study motivates further work, especially on the mechanical properties of the developing brain of mammals with gyrencephalic (folding) brains. Such data are needed to help evaluate the tension-based theory of cortical folding.

Acknowledgments We gratefully acknowledge technical assistance from Edward Kim, William McCarran, and Christine McDonald in harvesting the mouse brains used in this work. We also thank Paul Bridgman, Krikor Dikranian, Jeffrey Neil, and David Van Essen for their helpful discussions and suggestions. This work was supported by the National Science Foundation (grant #DMS-0540701).

References

Alexander GM, Deitch JS, Seeburger JL, Valle LD, Heiman-Patterson TD (2000) Elevated cortical extracellular fluid glutamate in transgenic mice expressing human mutant (G93A) Cu/Zn superoxide dismutase. J Neurochem 74:1666–1673. doi:10.1046/j.1471-4159.2000.0741666.x

Chada S, Lamoureux P, Buxbaum RE, Heidemann SR (1997) Cytomechanics of neurite outgrowth from chick brain neurons. J Cell Sci 110:1179–1186

Cheng S, Bilston LE (2007) Unconfined compression of white matter. J Biomech 40:117–124. doi:10.1016/j.jbiomech.2005.11.004

Coats B, Margulies SS (2006) Material properties of porcine parietal cortex. J Biomech 39:2521–2525. doi:10.1016/j.jbiomech.2005.07.020

Dennerll TJ, Lamoureux P, Buxbaum RE, Heidemann SR (1989) The cytomechanics of axonal elongation and retraction. J Cell Biol 109:3073–3083. doi:10.1083/jcb.109.6.3073

Drapaca C, Tenti G, Rohlf K, Sivaloganathan S (2006) A quasi-linear viscoelastic constitutive equation for the brain: application to hydrocephalus. J Elast 85:65–83. doi:10.1007/s10659-006-9071-3

Elkin BS, Azeloglu EU, Costa KD, Morrison B (2007) Mechanical heterogeneity of the rat hippocampus measured by atomic force microscope indentation. J Neurotrauma 24:812–822. doi:10.1089/neu.2006.0169

Faisal AA, White JA, Laughlin SB (2005) Ion-channel noise places limits on the miniaturization of the brain's wiring. Curr Biol 15:1143–1149. doi:10.1016/j.cub.2005.05.056

Fung YC (1993) Biomechanics: mechanical properties of living tissues. Springer, New York

Fung YC (1998) Biomechanics: motion, flow, stress, and growth. Springer, New York

Gefen A, Gefen N, Zhu QL, Raghupathi R, Margulies SS (2003) Age-dependent changes in material properties of the brain and braincase of the rat. J Neurotrauma 20:1163–1177. doi:10.1089/089771503770802853

Gefen A, Margulies SS (2004) Are in vivo and in situ brain tissues mechanically similar? J Biomech 37:1339–1352. doi:10.1016/j.jbiomech.2003.12.032

Georges PC, Miller WJ, Meaney DF, Sawyer ES, Janmey PA (2006) Matrices with compliance comparable to that of brain tissue select neuronal over glial growth in mixed cortical cultures. Biophys J 90:3012–3018. doi:10.1529/biophysj.105.073114

Hilgetag CC, Barbas H (2006) Role of mechanical factors in the morphology of the primate cerebral cortex. PLOS Comput Biol 2:146–159. doi:10.1371/journal.pcbi.0020022

Hilgetag CC, Barbas H (2005) Developmental mechanics of the primate cerebral cortex. Anat Embryol (Berl) 210:411–417. doi:10.1007/s00429-005-0041-5

Hrapko M, van Dommelen JAW, Peters GWM, Wismans JSHM (2006) The mechanical behaviour of brain tissue: large strain response and constitutive modelling. Biorheol 43:623–636

Kingsbury MA, Rehen SK, Contos JJA, Higgins CM, Chun J (2003) Non-proliferative effects of lysophosphatidic acid enhance cortical growth and folding. Nat Neurosci 6:1292–1299. doi:10.1038/nn1157

Kioussi C, Appu M, Lohr CV, Fischer KA, Bajaj G, Leid M et al (2007) Co-expression of myosin II regulatory light chain and the NMDAR1 subunit in neonatal and adult mouse brain. Brain Res Bull 74:439–451. doi:10.1016/j.brainresbull.2007.07.024

Kyriacou SK, Mohamed A, Miller K, Neff S (2002) Brain mechanics for neurosurgery: modeling issues. Biomech Model Mechanobiol 1:151–164. doi:10.1007/s10237-002-0013-0

Lamoureux P, Buxbaum RE, Heidemann SR (1989) Direct evidence that growth cones pull. Nature 340:159–162. doi:10.1038/340159a0

Lamoureux P, Ruthel G, Buxbaum RE, Heidemann SR (2002) Mechanical tension can specify axonal fate in hippocampal neurons. J Cell Biol 159:499–508. doi:10.1083/jcb.200207174

Larvaron P, Boespflug-Tanguy O, Renou JP, Bonny JM (2007) In vivo analysis of the post-natal development of normal mouse brain by DTI. NMR Biomed 20:413–421. doi:10.1002/nbm.1082

Miller K (1999) Constitutive model of brain tissue suitable for finite element analysis of surgical procedures. J Biomech 32:531–537. doi:10.1016/S0021-9290(99)00010-X

Miller K, Chinzei K (2002) Mechanical properties of brain tissue in tension. J Biomech 35:483–490. doi:10.1016/S0021-9290(01)00234-2

Miller K, Chinzei K, Orssengo G, Bednarz P (2000) Mechanical properties of brain tissue in-vivo: experiment and computer simulation. J Biomech 33:1369–1376. doi:10.1016/S0021-9290(00)00120-2

Miller K, Chinzei K (1997) Constitutive modelling of brain tissue: experiment and theory. J Biomech 30:1115–1121. doi:10.1016/S0021-9290(97)00092-4

Miller M, Bower E, Levitt P, Li D, Chantler PD (1992) Myosin II distribution in neurons is consistent with a role in growth cone motility but not synaptic vesicle mobilization. Neuron 8:25–44. doi:10.1016/0896-6273(92)90106-N

Neil J, Miller J, Mukherjee P, Huppi PS (2002) Diffusion tensor imaging of normal and injured developing human brain—a technical review. NMR Biomed 15:543–552. doi:10.1002/nbm.784

Nordahl CW, Dierker D, Mostafavi I, Schumann CM, Rivera SM, Amaral DG, et al (2007) Cortical folding abnormalities in autism revealed by surface-based morphometry. J Neurosci 27:11725–11735. doi:10.1523/JNEUROSCI.0777-07.2007

Olivares R, Montiel J, Aboitiz F (2001) Species differences and similarities in the fine structure of the mammalian corpus callosum. Brain Behav Evol 57:98–105. doi:10.1159/000047229

Porter BE, Brooks-Kayal A, Golden JA (2002) Disorders of cortical development and epilepsy. Arch Neurol 59:361–365. doi:10.1001/archneur.59.3.361

Prange MT, Margulies SS (2002) Regional, directional, and age-dependent properties of the brain undergoing large deformation. J Biomech Eng 124:244–252. doi:10.1115/1.1449907

Richman DP, Stewart RM, Hutchinson JW, Caviness VS Jr (1975) Mechanical model of brain convolutional development. Science 189:18–21. doi:10.1126/science.1135626

Rodriguez EK, Hoger A, McCulloch AD (1994) Stress-dependent finite growth in soft elastic tissues. J Biomech 27:455–467. doi:10.1016/0021-9290(94)90021-3

Sallet PC, Elkis H, Alves TM, Oliveira JR, Sassi E, de Castro CC et al (2003) Reduced cortical folding in schizophrenia: an MRI morphometric study. Am J Psychiatry 160:1606–1613. doi:10.1176/appi.ajp.160.9.1606

Taber LA (2007) Theoretical study of Beloussov's hyper-restoration hypothesis for mechanical regulation of morphogenesis. Biomech Model Mechanobiol. doi:10.1007/s10237-007-0106-x

Taber LA, Perucchio R (2000) Modeling heart development. J Elast 61:165–197. doi:10.1023/A:1011082712497

Taber LA (2001) Biomechanics of cardiovascular development. Annu Rev Biomed Eng 3:1–25. doi:10.1146/annurev.bioeng.3.1.1

Taylor Z, Miller K (2004) Reassessment of brain elasticity for analysis of biomechanisms of hydrocephalus. J Biomech 37:1263–1269. doi:10.1016/j.jbiomech.2003.11.027

Tekkok SB, Goldberg MP (2001) AMPA/kainate receptor activation mediates hypoxic oligodendrocyte death and axonal injury in cerebral white matter. J Neurosci 21:4237–4248

Thibault KL, Margulies SS (1998) Age-dependent material properties of the porcine cerebrum: effect on pediatric inertial head

injury criteria. J Biomech 31:1119–1126. doi:10.1016/S0021-9290(98)00122-5

Todd PH (1982) A geometric model for the cortical folding pattern of simple folded brains. J Theor Biol 97:529–538. doi:10.1016/0022-5193(82)90380-0

Toro R, Burnod Y (2005) A morphogenetic model for the development of cortical convolutions. Cereb Cortex 15:1900–1913. doi:10.1093/cercor/bhi068

Valverde F (2004) Golgi atlas of the postnatal mouse brain. Springer, New York

Van Essen DC (1997) A tension-based theory of morphogenesis and compact wiring in the central nervous system. Nature 385:313–318. doi:10.1038/385313a0

Welker W (1990) Why does cerebral cortex fissure and fold? A review of determinants of gyri and sulci. In: Jones EG, Peters A (eds) Cerebral cortex. Plenum, New York pp 3–136

Zamir EA, Taber LA (2004) On the effects of residual stress in microindentation tests of soft tissue structures. J Biomech Eng 126:276–283. doi:10.1115/1.1695573

Zhang LY, Yang KH, King AI (2001) Biomechanics of neurotrauma. Neurol Res 23:144–156. doi:10.1179/016164101101198488